

# Change-point Detection and Segmentation of Discrete Data using Bayesian Context Trees

Valentinian Lungu <sup>\*</sup>    Ioannis Papageorgiou <sup>†</sup>    Ioannis Kontoyiannis <sup>‡</sup>

January 14, 2025

## Abstract

A new Bayesian modelling framework is introduced for piecewise-homogeneous variable-memory Markov chains, along with a collection of effective algorithmic tools for change-point detection and segmentation of discrete time series. Building on the recently introduced Bayesian Context Trees (BCT) framework, the distributions of different segments in a discrete time series are described as variable-memory Markov chains. Inference for both the presence and location of change-points is then performed via Markov chain Monte Carlo sampling. The key observation that facilitates effective sampling is that the prior predictive likelihood in each segment of the data (averaged over all models and parameters) can be computed exactly. This makes it possible to sample directly from the posterior distribution of the number and location of the change-points, leading to accurate estimates and providing a natural quantitative measure of uncertainty in the results. Estimates of the actual model in each segment can also be obtained, at essentially no additional computational cost. Results on both simulated and real-world data indicate that the proposed methodology is robust and performs as well or better than state-of-the-art techniques.

**Keywords.** Discrete time series, change-point detection, segmentation, piecewise-homogeneous variable-memory chains, Bayesian context trees, context-tree weighting, Markov chain Monte Carlo, DNA segmentation.

---

<sup>\*</sup>Statistical Laboratory, Centre for Mathematical Sciences, University of Cambridge, Wilberforce Road, Cambridge CB3 0WB, UK. Email: [vm126@cam.ac.uk](mailto:vm126@cam.ac.uk).

<sup>†</sup>Department of Engineering, University of Cambridge, Trumpington Street, Cambridge CB2 1PZ, UK. Email: [ip307@cam.ac.uk](mailto:ip307@cam.ac.uk).

<sup>‡</sup>Statistical Laboratory, Centre for Mathematical Sciences, University of Cambridge, Wilberforce Road, Cambridge CB3 0WB, UK. Email: [yiannis@maths.cam.ac.uk](mailto:yiannis@maths.cam.ac.uk).

<sup>0</sup>Preliminary versions of some of the results in this paper were presented at the 2022 Information Theory Workshop ([Lungu et al., 2022](#)).

# 1 Introduction

Change-point detection and segmentation are important statistical tasks with a broad range of applications across the sciences and engineering. These tasks have been extensively studied in the case of real-valued time series; see, e.g., the reviews by [Aminikhanghahi and Cook \(2017\)](#); [Truong et al. \(2020\)](#); [van den Burg and Williams \(2020\)](#). A significant amount of work has also been done in addressing corresponding problems for discrete time series. Among the numerous applications there, e.g., in biomedicine, neuroscience, health system management, finance, and the social sciences ([Chandola et al., 2012](#)), the most critical application is probably the segmentation of genetic data, where the most commonly used tools are based on Hidden Markov Models (HMMs). Since their introduction for modelling heterogeneous DNA sequences by [Churchill \(1989, 1992\)](#), they have also become quite popular in a wide range of other disciplines as well ([Kehagias, 2004](#)). More recently, Bayesian HMM approaches have also been proposed and used in practice ([Boys and Henderson, 2004](#); [Totterdell et al., 2017](#)). In this paper we take a new Bayesian approach, based on modelling time series with change-points as piecewise-homogeneous variable-memory Markov chains.

As has been often noted, the two main obstacles in the direct approach to modelling dependence in discrete time series via ordinary, higher-order Markov chains, are that: (1). they form an inflexible and structurally poor model class; and (2). the number of parameters grows exponentially with the memory length. Variable-memory Markov chains provide a much richer and more flexible model class that offers parsimonious and easily interpretable representations of higher-order chains, by allowing the memory length to depend on the most recently observed symbols. These models were first introduced as *context-tree sources* in the information-theoretic literature ([Rissanen, 1983a,b, 1986](#)), where they have been used widely in connection with data compression. In particular, the development of the celebrated Context-Tree Weighting (CTW) algorithm ([Willems et al., 1995](#); [Willems, 1998](#)) is based on context-tree sources. Variable-memory Markov models were subsequently examined in the statistics literature, initially by [Bühlmann and Wyner \(1999\)](#) and [Mächler and Bühlmann \(2004\)](#), under the name Variable Length Markov Chains (VLMCs).

The present work is based in part on a Bayesian modelling framework, called Bayesian Context Trees (BCTs), which was recently developed by [Kontoyiannis et al. \(2022, 2021\)](#); [Kontoyiannis \(2024\)](#) and [Papageorgiou and Kontoyiannis \(2022, 2024\)](#) for the class of variable-memory Markov chains. The BCT framework allows for *exact* Bayesian inference (see Section 2), and it has been found to be very effective for inference with discrete time series. Moreover, it has also been extended to general Bayesian mixture models for real-valued time series ([Papageorgiou and Kontoyiannis, 2021, 2023](#)).

The first contribution of this work, in Section 3, is the introduction of a new Bayesian modelling framework for piecewise-homogeneous discrete time series. A uniform prior is placed on the number of change-points, and an “order statistics” prior is placed on their locations ([Green, 1995](#); [Fearnhead, 2006](#)), which penalizes short segments to avoid overfitting. Then each segment is described by a BCT model, thus defining a new class of *piecewise-homogeneous variable-memory chains*. Following [Kontoyiannis et al. \(2022\)](#), we observe that the models and parameters in each segment can be integrated out, and we explain how the corresponding prior predictive likelihoods can be computed exactly and efficiently by using a version of the CTW algorithm.

The second main contribution, also in Section 3, is the development of a new class of Bayesian methods for inferring the number and location of change-points in empirical data. A collection of appropriate Markov chain Monte Carlo (MCMC) algorithms is introduced, that sample directly and efficiently from the posterior distribution of the number and the locations of the change-points. The resulting approach is powerful as it provides an MCMC approximation for the entire posterior distribution of interest, offering broad and insightful information in addition to the estimates of the most likely change-points. Finally, in Section 4, the performance of our methods is illustrated on both simulated and real-world data from applications in genetics and meteorology, where they are found to perform at least as well as state-of-the-art approaches. All our algorithms are implemented in the publicly available R package BCT (Papageorgiou et al.), which also contains all relevant datasets.

**Further connections with earlier work.** Unlike many relevant existing methods that only obtain point estimates and may rely in part on *ad hoc* considerations, the present methodology comes from a principled Bayesian approach that provides access to the entire posterior distribution for the parameters of interest, in particular allowing for quantification of the uncertainty in the resulting estimates. The Bayesian approach was applied to the change-point detection problem in many influential works such as Adams and MacKay (2007), Barry and Hartigan (1993) or Fearnhead (2006); these works consider real-valued time series and they treat the observations within each segment as independent. In contrast, our model not only allows Markov dependency within each segment, but also works with both long and short memories through the BCT framework. The most closely related prior work is that of Gwadera et al. (2008), where VLMC models are used in conjunction with the BIC criterion (Schwarz, 1978) or with a variant of the Minimum Description Length principle (Rissanen, 1987) to estimate variable-memory models and perform segmentation by solving an associated Bellman equation.

There has also been a long line of works on change-point detection in the information-theoretic literature. There, piecewise-homogeneous models were first considered by Merhav (1993) and Merhav and Feder (1995), who determined the optimal cumulative log-loss (or ‘redundancy’, in the language of data compression). Starting with Willems (1996), a series of papers examined sequential change-point detection, typically (but not exclusively) for independent and piecewise identically distributed models. These works (Shamir and Merhav, 1999; Shamir and Costello, 2000, 2001; Shamir, 2003) are primarily concerned with deriving theoretical bounds on the best achievable performance by on-line methods, and also propose sequential algorithms for change-point detection, mostly for piecewise independent and identically distributed (i.i.d.) data. In a related but different direction, Jacob and Bansal (2008) and subsequently Juvvadi and Bansal (2013); Verma and Bansal (2019); Yamanishi and Fukushima (2018), frame the change-point detection problem as a series of hypothesis tests, performed using statistics based on data compression or entropy estimation algorithms. Similarly, Han et al. (2017), develop optimal Bayesian change-point detection tests for Markov processes. Although optimal, such tests are hard to use in practice. An approach combining HMMs with information-theoretic ideas is adopted in Koolen and de Rooij (2013), where prediction is performed on piecewise stationary data.

Finally, in the context of generalisations of the original CTW framework, change-point models have also been examined by Veness et al. (2012) and Veness et al. (2013), and more recently by Shimada et al. (2021), who consider optimal and practical ‘Bayes codes’ for data compression in connection with these models.

## 2 Background: Bayesian context trees

The BCT framework of [Kontoyiannis et al. \(2022\)](#), briefly outlined in this section, is based on variable-memory Markov chains, a class of models that offer parsimonious representations of  $D$ th order, homogeneous Markov chains taking values in a finite alphabet  $A = \{0, 1, \dots, m-1\}$ . The maximum memory length  $D \geq 0$  and the alphabet size  $m \geq 2$  are fixed throughout this section. Each model describes the distribution of a process  $\{X_n\}$  conditional on its initial  $D$  values  $X_{-D+1}^0 = x_{-D+1}^0$ , where we write  $X_i^j$  for a vector of random variables  $(X_i, X_{i+1}, \dots, X_j)$  and similarly  $x_i^j = (x_i, x_{i+1}, \dots, x_j)$  for a string in  $A^{j-i+1}$ . This is done by specifying the conditional distribution of each  $X_n$  given  $X_{n-D}^{n-1}$ .

The key step in the *variable-memory* model representation is the assumption that the distribution of  $X_n$  in fact only depends on a (typically strictly) shorter suffix  $x_{n-j}^{n-1}$  of  $x_{n-D}^{n-1}$ . All these suffixes, called *contexts*, can be collected into a proper  $m$ -ary tree  $T$  describing the *model* of the chain. [A tree here is called *proper* if all its nodes that are not leaves have exactly  $m$  children.] For example, consider the binary tree model on  $A = \{0, 1\}$  shown in Figure 1. With  $D = 3$ , given  $X_{n-3}^{n-1} = 111$ , the distribution of  $X_n$  only depends on the fact that the two most recent symbols are 1s, and it is given by the parameter  $\theta_{11}$ . In contrast, given  $X_{n-1}^{n-3} = 100$ , the distribution of  $X_n$  depends on all three recent symbols, and it is given by the parameter  $\theta_{100}$ .

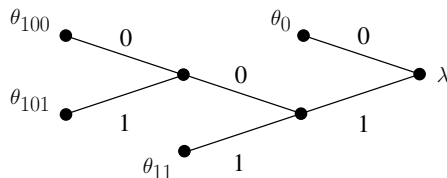


Figure 1: Tree model and parameters of a 3rd order variable-memory chain.

Let  $\mathcal{T}(D)$  denote the collection of all proper  $m$ -ary trees with depth no greater than  $D$ . To each leaf  $s$  of a model  $T \in \mathcal{T}(D)$ , we associate a probability vector  $\theta_s$  that describes the distribution of  $X_n$  given that the most recently observed context is  $s$ :  $\theta_s = (\theta_s(0), \theta_s(1), \dots, \theta_s(m-1))$ .

**Prior structure.** The prior distribution on models  $T \in \mathcal{T}(D)$  is given by,

$$\pi(T) = \pi_D(T; \beta) = \alpha^{|T|-1} \beta^{|T|-L_D(T)}, \quad (1)$$

where  $\beta \in (0, 1)$  is a hyperparameter,  $\alpha = (1 - \beta)^{1/(m-1)}$ ,  $|T|$  is the number of leaves of  $T$ , and  $L_D(T)$  is the number of leaves of  $T$  at depth  $D$ . This prior penalizes larger and more complex models by an exponential amount. Following the discussion in [Kontoyiannis et al. \(2022\)](#), the suggested default value of  $\beta = 1 - 2^{-m+1}$  is used throughout this paper.

Given a tree model  $T \in \mathcal{T}(D)$ , an independent  $\text{Dirichlet}(1/2, 1/2, \dots, 1/2)$  prior is placed on the parameters  $\theta = \{\theta_s : s \in T\}$  associated to the leaves  $s$  of  $T$ , so that,  $\pi(\theta|T) = \prod_{s \in T} \pi(\theta_s)$ , where,

$$\pi(\theta_s) = \pi(\theta_s(0), \theta_s(1), \dots, \theta_s(m-1)) \propto \prod_{j=0}^{m-1} \theta_s(j)^{-1/2}. \quad (2)$$

The extension to more general  $\text{Dirichlet}(\alpha_0, \dots, \alpha_{m-1})$  priors is straightforward ([Kontoyiannis et al., 2022](#)) and will not be considered here.

**Likelihood.** Given a tree model  $T \in \mathcal{T}(D)$  and associated parameters  $\theta = \{\theta_s : s \in T\}$ , the induced likelihood of a time series  $x = x_{-D+1}^n$  consisting of the observations  $x_1^n$  and initial context  $x_{-D+1}^0$ , is given by,

$$P(x|T, \theta) := P(x_1^n | T, \theta, x_{-D+1}^0) = \prod_{i=1}^n P(x_i | T, \theta, x_{-D+1}^{i-1}) = \prod_{s \in T} \prod_{j=0}^{m-1} \theta_s(j)^{a_s(j)}, \quad (3)$$

where, for each  $s \in T$ , the elements of the count vector  $a_s = (a_s(0), a_s(1), \dots, a_s(m-1))$  are:

$$a_s(j) := [\# \text{ times symbol } j \in A \text{ follows context } s \text{ in } x_1^n], \quad j \in A. \quad (4)$$

Observe that (3) is simply an instance of the Markov property.

**Marginal likelihood.** Given a tree model  $T \in \mathcal{T}(D)$ , it is possible to integrate out the parameters and compute the marginal likelihood  $P(x|T)$  of  $x = x_{-D+1}^n$  in closed form (Kontoyiannis et al., 2022):

$$P(x|T) := \int P(x_1^n | x_{-D+1}^0, T, \theta) \pi(\theta|T) = \prod_{s \in T} \frac{\prod_{j=0}^{m-1} (1/2)(3/2) \dots (a_s(j) - 1/2)}{(m/2)(m/2 + 1) \dots (m/2 + M_s - 1)},$$

where  $M_s = a_s(0) + a_s(1) + \dots + a_s(m-1)$  and the counts  $a_s(j)$  are defined in (4).

**Exact Bayesian inference.** An important property of the BCT framework is that it allows for *exact* Bayesian inference. In particular, for a time series  $x = x_{-D+1}^n$ , the prior predictive likelihood (or evidence)  $P_D^*(x)$ , averaged over both models and parameters, namely,

$$P_D^*(x) = \sum_{T \in \mathcal{T}(D)} \pi(T) \int_{\theta} P(x|T, \theta) \pi(\theta|T) d\theta,$$

can be computed *exactly* by the CTW algorithm (Kontoyiannis et al., 2022), despite the fact that the number of models in  $\mathcal{T}(D)$  is doubly exponential in  $D$ . Moreover, the BCT algorithm (Kontoyiannis et al., 2022) can be used to efficiently identify the *maximum a posteriori* probability (MAP) tree model.

### 3 BCT-based change-point detection

Here we describe the proposed Bayesian modelling framework for piecewise-homogeneous discrete time series, and the associated inference methodology for change-point detection.

Each segment is modelled by a homogeneous variable-memory chain as in Section 2. Two different cases are considered: When the number of change-points  $\ell$  is known *a priori*, and when  $\ell$  is unknown and needs to be inferred as well. Consider a time series  $x = x_{-D+1}^n$  consisting of the observations  $x_1^n$  along with their initial context  $x_{-D+1}^0$ . Let  $\ell$  denote the number of change-points and let  $1 = p_0 < p_1 < p_2 < \dots < p_\ell < p_{\ell+1} = n$  denote their locations, where we include the end-points  $p_0 = 1$  and  $p_{\ell+1} = n$  for convenience. We write,  $\mathbf{p} = (p_0, p_1, \dots, p_{\ell+1})$ .

### 3.1 Known number of change-points

**Piecewise homogeneous Markov models.** Suppose the maximum memory length  $D$  is fixed. Given a time series  $x = x_{-D+1}^n$ , the number of change-points  $\ell$ , and their locations  $\mathbf{p} = (p_0, p_1, \dots, p_{\ell+1})$ , the observations  $x_1^n$  are partitioned into  $(\ell + 1)$  segments,

$$\begin{aligned} x(1; \mathbf{p}) &= x_1^{p_1-1}, \\ x(j; \mathbf{p}) &= x_{p_{j-1}}^{p_j-1}, \text{ for } j = 2, 3, \dots, \ell, \\ x(\ell + 1; \mathbf{p}) &= x_{p_\ell}^n. \end{aligned}$$

Each segment  $x(j; \mathbf{p})$ ,  $1 \leq j \leq \ell + 1$ , is assumed to be distributed as a variable-memory chain with model  $T^{(j)} \in \mathcal{T}(D)$ , parameter vector  $\theta^{(j)}$ , and initial context given by the  $D$  symbols preceding  $x_{p_{j-1}}$  (i.e., the last  $D$  symbols of the previous segment). The resulting likelihood is,

$$P(x|\mathbf{p}, \{\theta^{(j)}\}, \{T^{(j)}\}) = \prod_{j=1}^{\ell+1} P(x_{p_{j-1}}^{p_j-1} | x_{p_{j-1}-D}^{p_j-1-1}, \theta^{(j)}, T^{(j)}),$$

where each term in the product is given by (3).

**Prior structure.** Given the number  $\ell$  of change-points, following Green (1995) and Fearnhead (2006), we place a prior on their locations  $\mathbf{p}$  specified by the even-order statistics of  $(2\ell + 1)$  uniform draws from  $\{2, 3, \dots, n - 1\}$  without replacement,

$$\pi(\mathbf{p}|\ell) = K_\ell^{-1} \prod_{j=0}^{\ell} (p_{j+1} - p_j - 1), \quad (5)$$

where  $K_\ell = \binom{n-2}{2\ell+1}$ . This prior penalizes short segments to avoid overfitting: The probability of  $\mathbf{p}$  is proportional to the product of the lengths of the segments  $x(j; \mathbf{p})$ . Finally, given  $\ell$  and  $\mathbf{p}$ , an independent BCT prior  $\pi(T^{(j)})\pi(\theta^{(j)}|T^{(j)})$  is placed on the tree-model and parameters of each segment  $j$ , as in (1) and (2).

**Posterior distribution.** The posterior distribution of the change-point locations  $\mathbf{p}$  is,

$$\pi(\mathbf{p}|x) \propto P(x|\mathbf{p})\pi(\mathbf{p}|\ell),$$

with  $\pi(\mathbf{p}|\ell)$  as in (5). To compute the term  $P(x|\mathbf{p})$ , all models  $T^{(j)}$  and parameters  $\theta^{(j)}$  in  $P(x, \{\theta^{(j)}\}, \{T^{(j)}\}|\mathbf{p})$  need to be integrated out. Since independent priors are placed on different segments,  $P(x|\mathbf{p})$  reduces to the product of the prior predictive likelihoods,

$$P(x|\mathbf{p}) = \prod_{j=1}^{\ell+1} P_D^*(x(j; \mathbf{p})), \quad (6)$$

where the dependence on the initial context for each segment is suppressed to simplify notation.

Importantly, each term in the product (6) can be computed efficiently using the CTW algorithm. This means that models and parameters in each segment can be marginalized out, making it possible to efficiently compute the unnormalised posterior distribution  $\pi(\mathbf{p}|x)$  for any  $\mathbf{p}$ . This is critical for effective inference on  $\mathbf{p}$ , as it means that there is no need to estimate or sample the variables  $\{T^{(j)}\}$  and  $\{\theta^{(j)}\}$  in order to sample directly from  $\pi(\mathbf{p}|x)$ , as described next.

**MCMC sampler.** The MCMC sampler for  $\pi(\mathbf{p}|x)$  is a Metropolis-Hastings (Robert and Casella, 2004) algorithm. It takes as input the time series  $x = x_{-D+1}^n$ , the alphabet size  $m \geq 2$ , the maximum memory length  $D \geq 0$ , the prior hyperparameter  $\beta$ , the number of change-points  $\ell \geq 1$ , the initial MCMC state  $\mathbf{p}^{(0)}$ , and the total number of MCMC iterations  $N$ .

Given the current state  $\mathbf{p}^{(t)} = \mathbf{p}$ , a new state  $\mathbf{p}'$  is proposed as follows: One of the change-points  $p_i$  is chosen at random from  $\mathbf{p}$  (excluding the edges  $p_0 = 1$  and  $p_{\ell+1} = n$ ), and it is replaced either by a uniformly chosen position  $p'_i$  from the  $(n - \ell - 2)$  remaining available positions, with probability  $1/2$ , or by one of its two neighbours, again with probability  $1/2$ . Note that the neighbours of a change-point are always available, as the prior places zero probability to adjacent change-points.

The proposed  $\mathbf{p}'$  is either accepted and  $\mathbf{p}^{(t+1)} = \mathbf{p}'$ , or rejected and  $\mathbf{p}^{(t+1)} = \mathbf{p}$ , where the acceptance probability is given by  $\alpha(\mathbf{p}, \mathbf{p}') = \min\{1, r(\mathbf{p}, \mathbf{p}')\}$ , where,

$$r(\mathbf{p}, \mathbf{p}') = \frac{P(x|\mathbf{p}')}{P(x|\mathbf{p})} \times \prod_{j=0}^{\ell} \frac{(p'_{j+1} - p'_j - 1)}{(p_{j+1} - p_j - 1)}.$$

We emphasise the fact that the terms  $P(x|\mathbf{p})$  and  $P(x|\mathbf{p}')$  can be computed efficiently by the CTW algorithm, which is what enables this sampler to work effectively.

This sampler is designed to allow for better exploration of the posterior distribution near change-points: First, the uniform jump moves of the sampler find a rough estimate of the location of a change-point, and then random-walk moves scan the region near the change-point to give an accurate picture of the posterior distribution around it.

### 3.2 Unknown number of change-points

The number  $\ell$  of change-points is often not known *a priori*, and needs to be treated as an additional parameter to be inferred. As before, given the number and location of the change-points, each segment is modelled by a variable-memory chain.

**Prior structure.** Given the maximum possible number of change-points  $\ell_{\max} \geq 1$ , we place a uniform prior for  $\ell$  on  $\{0, 1, \dots, \ell_{\max}\}$ , and, given  $\ell$ , the rest of the priors on  $\mathbf{p}$ ,  $\{T^{(j)}\}$  and  $\{\theta^{(j)}\}$  remain the same as in Section 3.1. The uniform prior is a common choice for  $\ell$  in such problems, as more complex models are implicitly penalised by averaging over a larger number of parameters, resulting in what is sometimes referred to as “automatic Occam’s Razor” (Smith and Spiegelhalter, 1980; Kass and Raftery, 1995; Rasmussen and Ghahramani, 2000).

**Posterior distribution.** The posterior distribution of the number and locations of the change-points is,

$$\pi(\mathbf{p}, \ell|x) \propto P(x|\mathbf{p}, \ell)\pi(\mathbf{p}|\ell)\pi(\ell), \quad (7)$$

where  $\pi(\mathbf{p}|\ell)$  is given in (5),  $\pi(\ell) = \frac{1}{1+\ell_{\max}}$ , and the term  $P(x|\mathbf{p}, \ell)$  is identical to  $P(x|\mathbf{p})$  in (6).

**MCMC sampler.** The MCMC sampler for  $\pi(\mathbf{p}, \ell|x)$  is again a Metropolis-Hastings algorithm. Given the current state  $(\ell^{(t)}, \mathbf{p}^{(t)}) = (\ell, \mathbf{p})$ , propose a new state  $(\ell', \mathbf{p}')$  as follows:

- (i) If  $\ell = 0$ , set  $\ell' = 1$ , choose  $p'_1$  uniformly in  $\{2, \dots, n - 1\}$ , and form  $\mathbf{p}' = (1, p'_1, n)$ .
- (ii) If  $1 \leq \ell < \ell_{\max}$ , then select one of the following three options with probability  $1/3$  each:
  - (a) Set  $\ell' = \ell - 1$  and form  $\mathbf{p}'$  by deleting a uniformly chosen change-point from  $\mathbf{p}^{(t)}$ ;



- (b) Set  $\ell' = \ell + 1$ , choose a new change-point uniformly from the  $(n - \ell - 2)$  available positions, and let  $\mathbf{p}'$  be the same as  $\mathbf{p}^{(t)}$  with the new point added;
  - (c) Set  $\ell' = \ell$  and propose  $\mathbf{p}'$  as in the sampler of Section 3.1.
- (iii) If  $\ell = \ell_{\max}$ , then select one of the following two options with probability 1/2 each:
- (a) Set  $\ell' = \ell - 1$  and form  $\mathbf{p}'$  by deleting a uniformly chosen change-point from  $\mathbf{p}^{(t)}$ ;
  - (b) Set  $\ell' = \ell$  and propose  $\mathbf{p}'$  as in the sampler of Section 3.1.

Finally, either accept  $(\ell', \mathbf{p}')$  and set  $(\ell^{(t+1)}, \mathbf{p}^{(t+1)}) = (\ell', \mathbf{p}')$ , or reject it and set  $(\ell^{(t+1)}, \mathbf{p}^{(t+1)}) = (\ell, \mathbf{p})$ , with acceptance probability  $\alpha((\ell, \mathbf{p}), (\ell', \mathbf{p}')) = \min\{1, r((\ell, \mathbf{p}), (\ell', \mathbf{p}'))\}$ , where, in view of (7), the ratio  $r((\ell, \mathbf{p}), (\ell', \mathbf{p}'))$  can again be computed easily via the CTW algorithm; the exact form of  $r((\ell, \mathbf{p}), (\ell', \mathbf{p}'))$  is given in Appendix A.

## 4 Experimental results

In this section, we evaluate the performance of the proposed BCT-based methods for segmentation and change-point detection described in the previous section, and we compare them with other state-of-the-art approaches on simulated data and real-world time series from applications in genetics and meteorology.

The only free parameters in the application of the BCT-based methods are the model prior parameter  $\beta \in (0, 1)$ , the maximum memory length  $D \geq 0$ , and the maximum number of change-points  $\ell_{\max} \geq 1$ . In the experiments in this section we use the recommended (Kontoyiannis et al., 2022) default value of  $\beta = 1 - 2^{-m+1}$ . The memory length  $D$  is selected by the modeller, depending on the length of the data and the prior understanding about the statistical nature of the observations; we use the values  $D = 3, 5$  and 10. Finally,  $\ell_{\max}$  should generally be chosen at least as large as the maximum possible number of change-points potentially present in the data.

In our experiments it was found that the results were quite insensitive to the particular choices for these three parameters, as long as their values were not rather obviously unreasonable. Further discussion about the finer points of the choice of  $\beta$  and  $D$  is given in Kontoyiannis et al. (2022), and about the choice of  $\ell_{\max}$  in Section 4.2.2.

### 4.1 Known number of change-points

For the simpler problem when the number of change-points is known *a priori*, here we examine the performance of the BCT-based change-point detection method of Section 3.1 on a standard benchmark data set from statistical genetics.

The Simian virus 40 (SV40) is one of the most extensively studied animal viruses. Its genome is a circular double-stranded DNA molecule of 5243 base-pairs (Reddy et al., 1978), available as sequence NC.001669.1 at the GenBank database (Clark et al., 2016). The expression of SV40 genes is regulated by two major transcripts (early and late), suggesting the presence of a single major change-point in the entire genome (Churchill, 1992; Totterdell et al., 2017; Rotondo et al., 2019). One transcript is responsible for producing structural virus proteins while the other one is responsible for producing two T-antigens (a large and a small one). Hence, we take the start of the gene producing the large T-antigen to be the “true” change-point of the dataset, corresponding to position  $p_1^* = 2691$ .



The MCMC sampler of Section 3.1 was run with  $\ell = 1$  and  $D = 10$ . The left plot in Figure 2 shows the resulting histogram of the change-point  $p_1$ , between locations 2800 and 2880; there were essentially no MCMC samples outside that interval. Viewing this as an approximation to the posterior distribution  $\pi(p_1|x)$ , the approximate MAP location  $\hat{p}_1 = 2827$  is obtained.

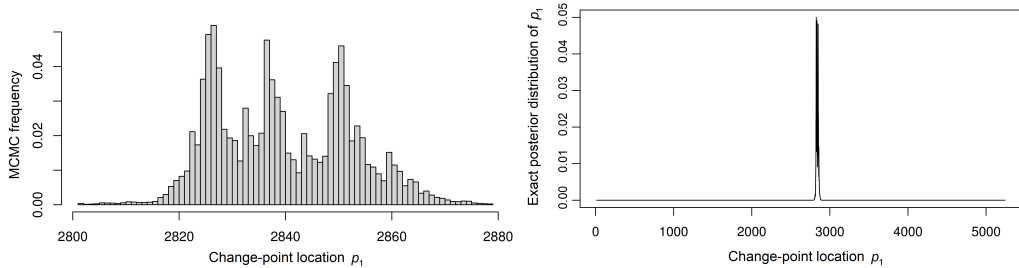


Figure 2: Posterior distribution  $\pi(p_1|x)$  of the change-point location for the SV40 genome. Left: MCMC histogram of  $\pi(p_1|x)$  near its mode based on  $N = 300,000$  MCMC samples, with the first 30,000 discarded as burn-in. Right: Entire exact posterior distribution,  $\pi(p_1|x)$ .

Compared to the results of two of the standard, state-of-the-art methods, our estimate  $\hat{p}_1$  is slightly closer to  $p_1^*$  than that produced by the HMM-based technique of Churchill (1992) which gives  $\hat{p}_1 \approx 2859$ , and that of the Bayesian HMM approach by Totterdell et al. (2017) which gives  $\hat{p}_1 \approx 2854$ . Moreover, the BCT-based algorithm is a general-purpose method that is agnostic with respect to the nature of the observations; unlike many earlier approaches, it does not utilise any biological information about the structure of the data.

Since this dataset is relatively short and contains a single change-point, it is actually possible to compute the entire posterior distribution of the location  $p_1$  exactly, through,

$$\pi(p_1|x) = \frac{P(x|p_1)\pi(p_1|\ell = 1)}{\sum_{p=2}^{n-1} P(x|p)\pi(p|\ell = 1)}.$$

Here,  $\pi(p_1|\ell = 1)$  is given by (5), and the terms  $P(x|p_1)$  and  $P(x|p)$  in the numerator and denominator can be computed through  $n - 2$  applications of the CTW algorithm. The resulting exact posterior distribution is shown in the right plot in Figure 2 and in more detail in Figure 3. Even though the shape of the posterior distribution around the mode is quite irregular, the MCMC estimate is almost identical to the true distribution. This indicates that the MCMC sampler converges quite fast and explores all of the support of  $\pi(p_1|x)$  effectively.

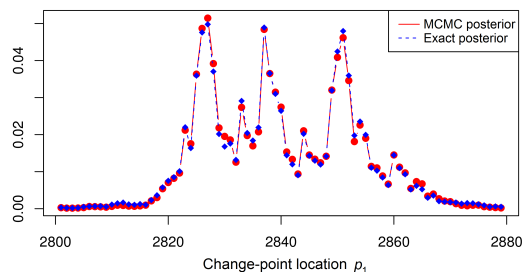


Figure 3: Exact distribution vs. MCMC histogram of  $\pi(p_1|x)$  based on  $N = 300,000$  MCMC samples, for the SV40 genome.

In addition to a point estimate for  $p_1^*$ , the posterior distribution also identifies an interval in which  $p_1^*$  likely lies, illustrating a common advantage of the Bayesian approach. We also note that, the fact that the posterior distribution here can be computed without resorting to MCMC, does not simply indicate that MCMC sampling is sometimes unnecessary. It actually highlights the power of the marginalization provided by the CTW algorithm in that, for relatively short datasets with few change-points, it is possible to obtain the entire *exact* posterior distribution.

## 4.2 Unknown number of change-points

In this section we illustrate the application of the BCT-based change-point detection method of Section 3.2 for the more interesting case when the number of change-points is *a priori* unknown, and we compare its performance with existing state-of-the-art techniques. In Sections 4.2.1–4.2.4 we examine various aspects of the change-point detection problem using appropriately simulated data, and in Sections 4.2.5 and 4.2.6 we look at real-world datasets from genetics and meteorology.

### 4.2.1 False alarms

An important aspect of change-point detection tasks is the potential occurrence of false positives, that is, instances where a change-point is erroneously detected in data where no genuine change exists. Here we investigate how the BCT-based method behaves with homogeneous data. We consider three simple generating distributions: i.i.d. data uniformly distributed over  $\{0, 1, 2, 3\}$ , i.i.d. Bernoulli data with parameter 0.2, and data generated by a binary variable-memory Markov chain with contexts “0”, “10” and “11” and associated parameters:  $P(1|0) = 1 - P(0|0) = 0.8$ ,  $P(1|10) = 1 - P(0|10) = 0.1$ , and  $P(1|11) = 1 - P(0|11) = 0.5$ . The total number of observations was varied from  $n = 75$  to  $n = 1000$ , and the algorithm was ran with a maximum depth  $D = 3$  and  $\ell_{\max} = 2$ . The posterior distribution of the number of change-points is displayed in Table 1.

$n$	Posterior distribution of the number of change-points			
	75	100	500	1000
i.i.d. uniform	( <b>0.67</b> , 0.25, 0.08)	( <b>0.79</b> , 0.14, 0.07)	( <b>0.96</b> , 0.03, 0.01)	( <b>0.98</b> , 0.02, 0)
i.i.d. Bernoulli	( <b>0.70</b> , 0.20, 0.10)	( <b>0.82</b> , 0.15, 0.03)	( <b>0.90</b> , 0.08, 0.02)	( <b>0.95</b> , 0.05, 0)
Markov chain	( <b>0.70</b> , 0.20, 0.10)	( <b>0.85</b> , 0.08, 0.07)	( <b>0.97</b> , 0.02, 0.01)	( <b>0.99</b> , 0.01, 0)

Table 1: The posterior distribution of the number of change-points for three simulated datasets. Each entry contains the vector of estimated posterior probabilities  $\pi(\ell|x)$  of having  $\ell = 0, 1$ , or 2 change-points. In all cases,  $N = 10^4$  MCMC iterations were performed, with the first 2,000 samples being discarded as burn-in.

The results indicate that the BCT-based algorithm correctly assigns most of the posterior mass to  $\ell = 0$  change-points and, as the number of observations grows, the posterior distribution  $\pi(\ell|x)$  becomes more confident in the absence of change-points.

### 4.2.2 The choice of $\ell_{\max}$

Here we examine how the behaviour of the BCT-based method changes when the parameter  $\ell_{\max}$  is varied. The first dataset we consider is made up of three segments of length 100 samples each; the first segment consists of i.i.d. Bernoulli data with parameter 0.8, the second is generated by

the simple binary variable-memory chain in the previous section, and the third contains i.i.d. Bernoulli samples with parameter 0.5. The second dataset we consider has the same distribution, but each segment now contains 300 observations.

The results of the algorithm executed with  $D = 3$  and  $1 \leq \ell_{\max} \leq 4$  are given in Table 2. They show that, if  $\ell_{\max}$  is smaller than the true number of change-points  $\ell^* = 2$ , the posterior distribution places all its mass on  $\ell = \ell_{\max}$ , whereas if  $\ell_{\max} \geq \ell^*$  then it concentrates on the true value  $\ell = \ell^*$  and gives zero or very small probability on strictly smaller values of  $\ell$ . Note that, in contrast with Fearnhead (2006), Adams and MacKay (2007) or Barry and Hartigan (1993), we place a uniform prior on the number of change-points. Nevertheless, the posterior distribution does not overfit and is able to capture the correct number of change-points.

$\ell_{\max}$	Posterior distribution of the number of change-points			
	1	2	3	4
dataset 1	(0, <b>1</b> )	(0, 0.07, <b>0.93</b> )	(0, 0, <b>0.6</b> , 0.4)	(0, 0, <b>0.51</b> , 0.35, 0.14)
dataset 2	(0, <b>1</b> )	(0, 0, <b>1</b> )	(0, 0, <b>0.75</b> , 0.25)	(0, 0, <b>0.72</b> , 0.22, 0.06)

Table 2: The posterior distribution  $\pi(\ell|x)$  of the number of change-points, estimated from the two datasets in Section 4.2.2, based on  $N = 10^4$  MCMC iterations with the first 2,000 samples being discarded as burn-in. Each entry in the table corresponds to  $\pi(\ell|x)$  for  $\ell = 0, 1, \dots, \ell_{\max}$ .

Next, we examine the performance of the BCT-based method when  $\ell_{\max}$  is significantly larger than the true number of change-points. For the first dataset, taking  $\ell_{\max} = 25, 100, 250, 293$ , and initialising the sampler at the worst possible value,  $\ell^{(0)} = \ell_{\max}$ , the mode of the posterior distribution is still clearly at the correct value  $\ell = 2$ . Very similar results are obtained on the the second dataset with  $\ell_{\max} = 10, 150, 300, 600$ ; see Figures 13 and 12 in Appendix B.

Table 4 in Appendix C shows the behaviour of running time as a function of  $\ell_{\max}$ .

### 4.2.3 A ‘difficult’ simulated data set

We examine a synthetic dataset of length  $n = 4300$  samples, consisting of four different segments generated from four variable-memory chains with values in  $A = \{0, 1, 2\}$ ; the corresponding tree models are shown in Figure 4. The associated parameters, given in Appendix D, are chosen to be quite similar, so that the resulting segmentation problem is ‘difficult’. The locations of the three change-points are  $p_1^* = 2500$ ,  $p_2^* = 3500$ ,  $p_3^* = 4000$ .

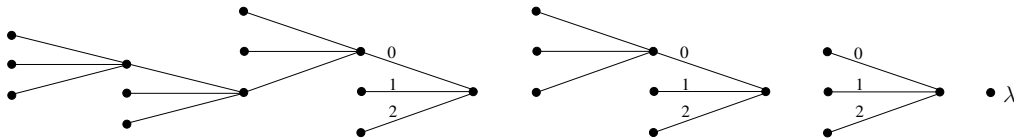


Figure 4: Four tree models of variable-memory Markov chains on  $A = \{0, 1, 2\}$  used for generating simulated data in Section 4.2.3. The last model is the empty tree consisting of only the root node  $\lambda$ , corresponding to i.i.d. data.

The MCMC sampler of Section 3.2 was run with  $\ell_{\max} = 5$  and  $D = 5$ ; see Figure 5.

The posterior distribution of the number of change-points identifies the correct value  $\ell = 3$  with overwhelming confidence. Similarly, the posterior distribution of the change-point locations

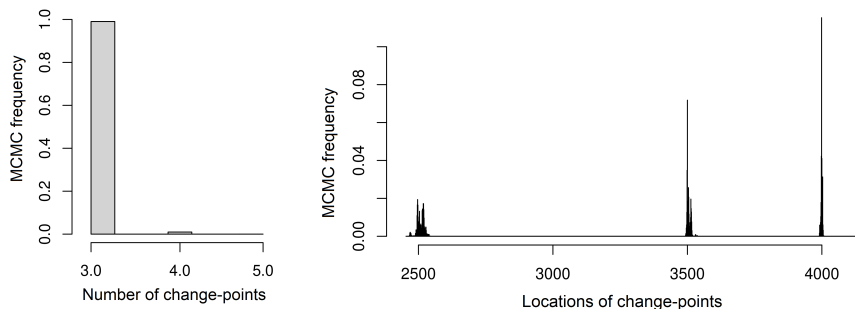


Figure 5: Simulated data. Left: MCMC histogram of the posterior distribution of the number of change-points. Right: MCMC histogram of the posterior distribution of the change-point locations. In both cases,  $N = 10^5$  MCMC iterations were performed, with the first 10,000 samples discarded as burn-in.

consists of three narrow peaks centered at the true locations. The MAP estimates for the change-point locations are  $\hat{p}_1 = 2497$ ,  $\hat{p}_2 = 3500$ ,  $\hat{p}_3 = 3999$ . Zoomed-in versions, showing the posterior distribution of the location of the three change-points, are shown in Figure 14 in Appendix E.

#### 4.2.4 Comparisons to previous work

In this slightly more extensive section, we carefully compare the performance of the BCT-based method with that of one of the state-of-the-art algorithms used in probabilistic DNA sequencing, the Bayesian HMM approach of [Totterdell et al. \(2017\)](#). We first examine two datasets simulated from an HMM, and then two datasets generated by an piecewise-homogeneous variable-memory chain.

**HMM data.** First we examine two simulated datasets generated by the following HMM whose parameters are the same as those used in [Totterdell et al. \(2017\)](#). The hidden state process  $\{S_n\}$  is a first-order Markov chain with values in  $\{1, 2\}$  and transition matrix,

$$\Lambda = \begin{bmatrix} 0.995 & 0.005 \\ 0.005 & 0.995 \end{bmatrix}.$$

The observed process  $\{X_n\}$  takes values in  $A = \{0, 1, 2, 3\}$  and evolves as follows: The conditional distribution of  $X_n$  given the value of the current state  $S_n = k$  and the preceding value of  $X_{n-1} = i$ , is generated according to the transition matrix  $P^{(k)} = (P_{ij}^{(k)})$ , where, for  $k = 1, 2$ :

$$P^{(1)} = \begin{bmatrix} 0.20 & 0.30 & 0.30 & 0.20 \\ 0.22 & 0.38 & 0.07 & 0.33 \\ 0.23 & 0.27 & 0.32 & 0.18 \\ 0.19 & 0.31 & 0.29 & 0.21 \end{bmatrix} \quad P^{(2)} = \begin{bmatrix} 0.35 & 0.15 & 0.15 & 0.35 \\ 0.37 & 0.13 & 0.13 & 0.37 \\ 0.32 & 0.18 & 0.10 & 0.40 \\ 0.35 & 0.20 & 0.20 & 0.25 \end{bmatrix}.$$

Both datasets have length  $n = 1000$ . The first has a single change-point (that is, a single state transition) at  $p_1^* = 412$ , while the second one has three, at  $p_1^* = 83$ ,  $p_2^* = 657$ , and  $p_3^* = 862$ .

Following [Boys and Henderson \(2004\)](#), in the Bayesian HMM approach of [Totterdell et al. \(2017\)](#), independent Dirichlet priors are placed on each row of the transitions matrices, so that the posterior distribution of the parameters  $P^{(1)}$ ,  $P^{(2)}$  and  $\Lambda$  can easily be obtained. Then the posterior distribution of the state sequence is estimated through a forward-backward algorithm.

For each simulated dataset, this Bayesian HMM algorithm was ran for 110,000 iterations by initialising the parameters as described in [Totterdell et al. \(2017\)](#). Our proposed change-point detection algorithm was ran for 110,000 MCMC iterations, with  $\ell_{\max} = 5$  and  $D = 3$ . The results are shown in Figures 6 and 7.

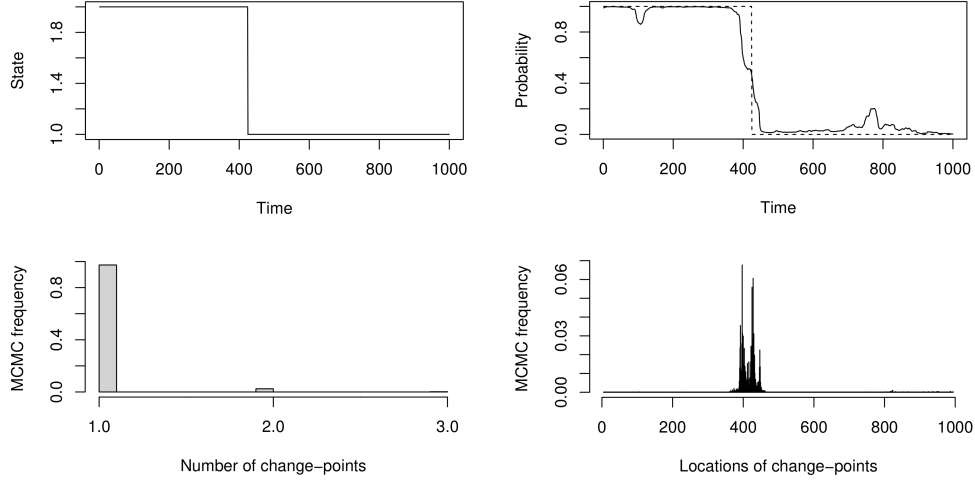


Figure 6: Top left: Hidden state sequence with a change-point at  $p_1^* = 412$ . Top right: Estimated segment probability,  $\pi(S_k = 1|x)$ ,  $1 \leq k \leq n$ ; true state sequence shown as the dashed line. Bottom: MCMC histograms of the posterior distribution of the number of change-points (left) and of the posterior distribution of the change-points locations (right).

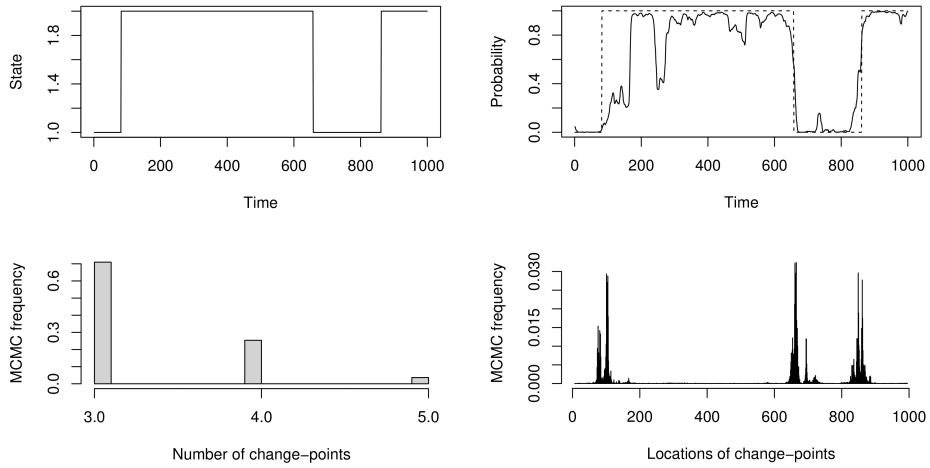


Figure 7: Top left: Hidden state sequence with change-points at  $p_1^* = 83$ ,  $p_2^* = 657$ ,  $p_3^* = 862$ . Top right: Estimated segment probability,  $\pi(S_k = 1|x)$ ,  $1 \leq k \leq n$ ; true state sequence shown as the dashed line. Bottom: MCMC histograms of the posterior distribution of the number of change-points (left) and of the posterior distribution of the change-points locations (right).

Despite the fact that the data were generated by a model that does not belong to the class of piecewise-homogeneous variable-memory chains, the BCT-based algorithm performs essentially

as well as the Bayesian HMM method in identifying the number and locations of the change-points. In addition, the BCT-based algorithm provides quantitative confidence estimates in the results obtained, and it also more flexible in terms of prior knowledge: The Bayesian HMM approach requires the specification of the exact number of hidden states, whereas the BCT-based method only needs the specification of the much less critical parameter  $\ell_{\max}$ .

Finally, due to the efficiency of the CTW and MCMC sampling algorithms, the proposed method algorithm was faster than the Bayesian HMM algorithm by at least 2 orders of magnitude; see the first two rows of Table 5 in Appendix C.

**Variable-memory chain data.** Next, we examine two data sets generated by piecewise-homogeneous variable-memory chains. Each dataset has length  $n = 2000$  samples, taking values in  $A = \{0, 1, 2\}$ , with a single change-point at  $p_1^* = 1000$ . In each case, the two segments are generated by variable-memory chains with respect to the two models shown in Figure 8; the associated parameters are given in Appendix D. In Figure 9, the results of the Bayesian HMM method are compared with those of the BCT-based algorithm with  $\ell_{\max} = 3$  and  $D = 5$ .

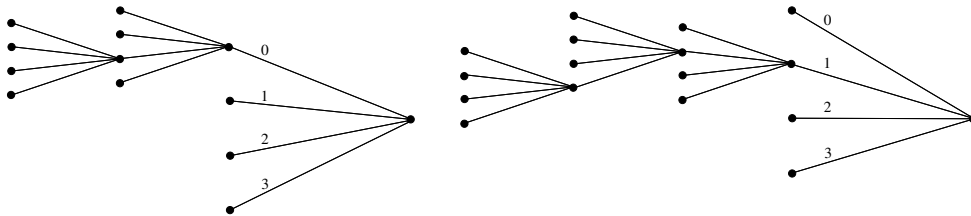


Figure 8: The models used for the variable-memory Markov chain datasets in Section 4.2.4.

For the first dataset (left column), the empirical HMM-estimated probability of being in state 1 gives no information on the location of the change-point, whereas the BCT-based algorithm both correctly identifies the presence of a single change-point and provides an accurate estimate of its location in the vicinity of positions 950-1000. For the second dataset (right column), the empirical HMM-estimated probability is smoother and correctly indicates the location of the change-point, but it also incorrectly identifies two non-existent changes. The BCT-based method again correctly identifies the presence of a single change point as well as its location.

Unlike the robustness demonstrated by the BCT-based method on HMM data, the Bayesian HMM method appears to not be robust when used on data generated by a process outside the HMM model class. Also, as before, the running time of the Bayesian HMM algorithm was found to be at least 100 times longer than that of the BCT-based algorithm; see Table 5 in Appendix C.

#### 4.2.5 Bacteriophage lambda

Here we revisit the 48,502 base-pair-long genome of the bacteriophage lambda virus (Sanger et al., 1982), available as sequence NC\_001416.1 at the GenBank database. This dataset is often used as a benchmark for comparing different segmentation algorithms (Churchill, 1989, 1992; Braun and Müller, 1998; Braun et al., 2000; Li, 2001; Boys and Henderson, 2004; Gwadera et al., 2008). Due to the high complexity of this genome, which consists of 73 different genes, previous approaches often give different results on both the number and locations of change-points, although all of them have been found to be biologically reasonable. For example, Gwadera et al. (2008) identify a total of 4 change-points, Li (2001); Boys and Henderson (2004) identify 5,

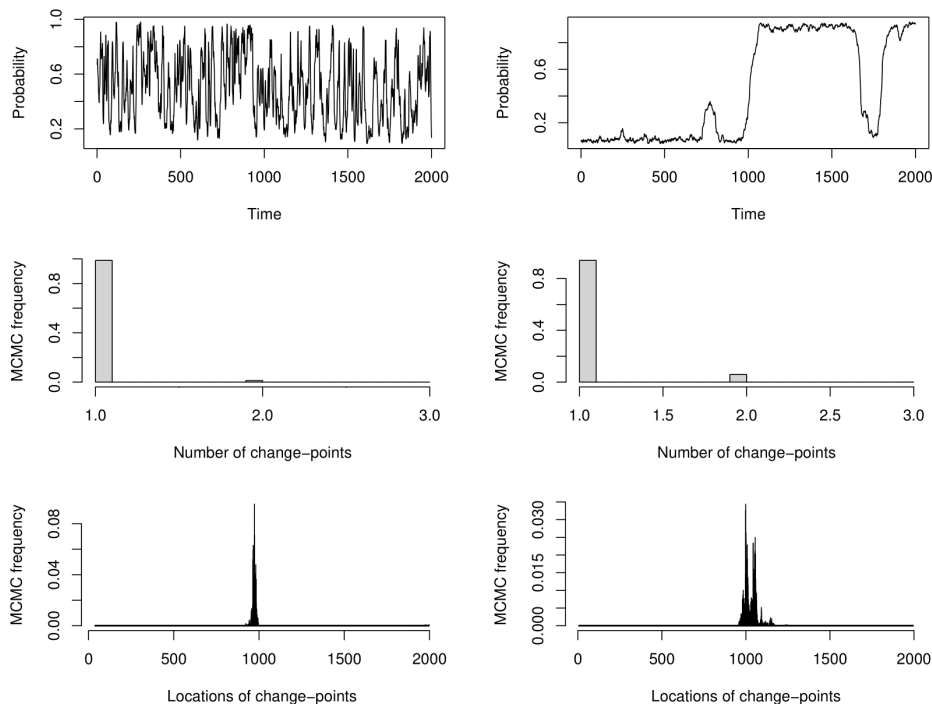


Figure 9: Results of the Bayesian HMM approach and the BCT-based change-point detection method, on two simulated datasets (one in each column) generated from variable-memory Markov chains, with a single change-point at  $p_1^* = 1000$ . For both algorithms, the same number  $N = 110,000$  of iterations were performed.

Churchill (1992); Braun and Müller (1998) identify 6, and Braun et al. (2000) identify 8 change-points. These differences make it difficult to compare the performance of different methods quantitatively, but judging the biological relevance of the identified segments is still crucial. In order to do so, we will refer to the findings in the standard biological reference work of Liu et al. (2013).

The MCMC sampler of Section 3.2 was run with  $D = 10$  and  $\ell_{\max} = 10$ . The resulting MCMC histogram approximation of the posterior distribution over the number of change-points (Figure 10, left plot) suggests that, with very high probability, there are either  $\ell = 4$  or 5 change-points, with  $\ell = 4$  being over seven times more likely than  $\ell = 5$ .

The posterior distribution of the change-point locations (Figure 10, right plot) clearly identifies four significant locations, as well as two more, around positions 100 and 24,000, with significantly smaller weights. Zoomed-in versions, showing the posterior distribution around each of the four main locations are given in Figure 15 in Appendix E. The resulting MAP estimates for the change-point locations are shown in Table 3, where they are also compared with the biologically “true” change-points according to Liu et al. (2013), and with the estimates provided by one of the most reliable, state-of-the-art methods that have been applied to this data (Braun et al., 2000). It is noted that the high computational requirements associated with this example make the use of the software by Totterdell et al. (2017) prohibitive in this case: Compared to the datasets considered in Section 4.2.4, the present dataset is two orders of magnitude larger, and one would need to consider at least  $r = 5$  hidden states.



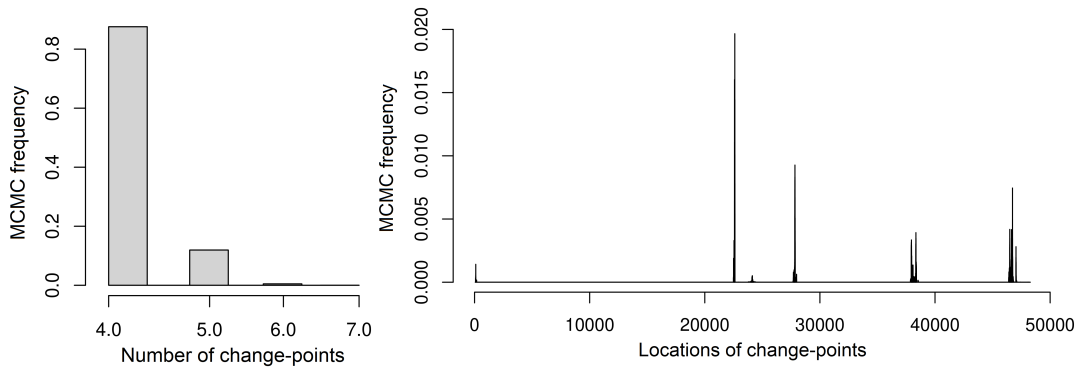


Figure 10: Posterior distribution of the number and location of change-points in the bacteriophage genome. Left: MCMC histogram of the posterior distribution of the number of change-points. Right: MCMC histogram of the posterior distribution of the change-point locations. In both cases,  $N = 700,000$  MCMC samples were obtained, with the first 70,000 discarded as burn-in.

According to [Liu et al. \(2013\)](#), the segments we identify correspond to a biologically meaningful and important partition in terms of gene expression. The first segment (1-22607) starts at the beginning of the genome and ends very close to the start of gene “ea47” (position 22686), which signifies the end of the “late operon” and the beginning of the leftward “early operon”, both of which play an important role in transcription. The second segment (22608-27832) essentially consists of the region “b2”, an important region containing the three well-recognized “early” genes “ea47”, “ea31” and “ea59”. The third segment (27833-38340) ends very close to the end of gene “cro” (position 38315), which is the start of the rightward “early operon” that is also essential in transcription. Lastly, the fourth segment (38341-46731) ends very close to the end (position 46752) of gene “bor”, one of the major genes being translated.

Gene	True	BCT	<a href="#">Braun et al. (2000)</a>
ea47	22686	<b>22607</b>	22544
ea59	26973	<b>27832</b>	27829
cro	38315	<b>38340</b>	38029
bor	46752	<b>46731</b>	46528

Table 3: Estimates of change-point locations in the bacteriophage lambda genome.

Compared with previous findings, our results are similar enough to be plausible, while the places where they differ are precisely in the identification of biologically meaningful features, potentially improving performance. Specifically, our estimates are very close to those obtained by [Gwadera et al. \(2008\)](#), where an approach based on variable-memory Markov models is also used: Four change-points are identified by [Gwadera et al. \(2008\)](#), and their estimated locations lie inside the credible regions of our corresponding posterior distributions.

Compared with the alternative Bayesian approach of [Boys and Henderson \(2004\)](#), the present method gives similar locations and also addresses some of the known limitations of the Bayesian HMM approach. First, it was noted earlier that the Bayesian HMM framework is sensitive to the assumed prior distribution on the hidden state transition parameters. In contrast, the BCT-based framework avoid this problem by relying on the prior predictive likelihood (which

marginalizes over all models and parameters), using a simple default value for the only prior hyperparameter,  $\beta$ . Also, as argued by Gupta and Liu (2004), the assumption that all segments share the same memory length may be problematic for the HMM approach. The BCT-based methodology requires no such assumptions and, indeed, allows for the memory length of each segment to vary arbitrarily. For example, the MAP tree models obtained by the BCT algorithm in each segment of this dataset have maximum depths  $d = 5, 1, 2, 3$  and  $0$ , respectively, indicating that the memory length indeed varies throughout the genome.

#### 4.2.6 El Niño

El Niño (Trenberth, 1997) is one of the most influential natural climate patterns on earth. It impacts ocean temperatures, the strength of ocean currents, and the local weather in South America. As a result, it has direct societal consequences on areas including the economy (Cashin et al., 2017) and public health (Kovats et al., 2003). Moreover, studying the frequency change of El Niño events can shed light on anthropogenic warming (Timmermann et al., 1999; Cai et al., 2014; Wang et al., 2019). The dataset considered here is a binary time series that consists of 495 annual observations between 1525 to 2020 (Quinn et al., 1987), with 0 representing the absence of an El Niño event and 1 indicating its presence; data for recent years are also available online through the US Climate Prediction Center, at: [https://origin.cpc.ncep.noaa.gov/products/analysis\\_monitoring/ensostuff/ONI\\_v5.php](https://origin.cpc.ncep.noaa.gov/products/analysis_monitoring/ensostuff/ONI_v5.php).

The MCMC sampler of Section 3.2 was run with  $D = 5$  and  $\ell_{\max} = 5$ . The resulting MCMC estimate of the posterior distribution on the number of change-points (left plot in Figure 11) suggests that the most likely value is  $\ell = 2$ , with  $\ell = 1$  being a close second. The posterior distribution of the change-point locations (right plot in Figure 11) also shows two clear peaks; zoomed-in versions showing the location of each change-point separately are given in Figure 16 in Appendix E.

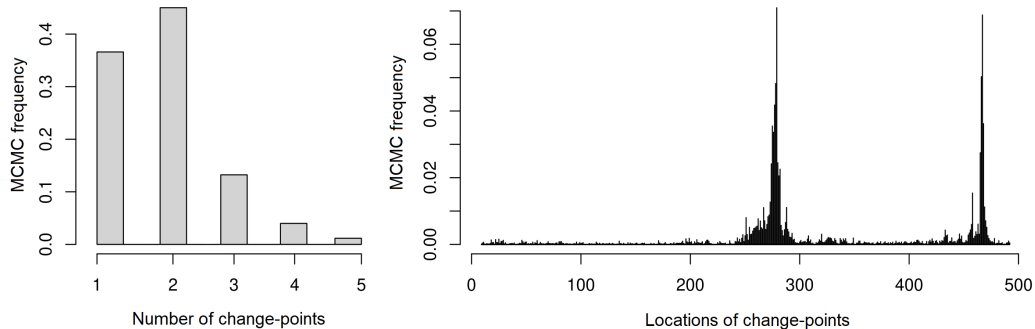


Figure 11: Posterior distribution of the number and location of the change-points for the El Niño dataset. Left: MCMC histogram of the posterior distribution of the number of change-points. Right: MCMC histogram of the posterior distribution of the change-point locations. In both cases,  $N = 20,000$  iterations were performed and the first 2,000 samples were discarded as burn-in.

The MAP estimates of the two locations are at  $\hat{p}_1 = 278$  and  $\hat{p}_2 = 467$ , corresponding to historically meaningful events during the years 1802 and 1991, respectively: The first change-point can be attributed to advancements in recording meteorological events, as prior to 1800 only

the strong and extreme events were recorded (Quinn et al., 1987). The second change-point in the early 1990s likely indicates a response to greenhouse warming, which is expected to increase both the frequency and the intensity of El Niño events (Cai et al., 2014; Timmermann et al., 1999). Indeed, examining the first-order marginal  $\pi = (\pi(0), \pi(1))$  of the stationary distribution associated with the MAP tree model in each segment, we find that the frequency  $\pi(1)$  of the recorded El Niño events increases between consecutive segments, from  $\pi(1) = 0.14$  before 1802, to  $\pi(1) = 0.35$  between 1802 and 1991, and finally to  $\pi(1) = 0.54$  after 1991.

## 5 Conclusions

In this work, a new hierarchical Bayesian framework was developed for change-point detection and segmentation of discrete time series, based on the BCT family of models and algorithms. First, a new model class of piecewise-homogeneous variable-memory Markov chains was described, and then an associated collection of algorithmic tools for segmentation and change-point detection was introduced.

The new BCT-based methods are practical MCMC algorithms that only sample from the posterior distribution of the parameters of interest: The number of change points and their locations. The fact that all other parameters and models can be integrated out (by employing the CTW algorithm) results in computationally efficient samplers that were found to be at least 100 times faster than other state-of-the-art techniques we compared with. These MCMC samplers incorporate uniform random jumps that identify the approximate positions of change-points, as well as short-range random-walk moves that explore the high-probability regions around them. This way, the entire state space is explored effectively, providing an accurate estimate of the desired posterior distribution.

An important advantage of the proposed tools is that they are based on a principled Bayesian approach, leading to general-purpose and application-agnostic methods that do not require any prior information on the nature of the data. They are robust with respect to the underlying parameter choices and, unlike earlier Bayesian-HMM approaches, they do not require additional prior information on the number of underlying states.

In numerous experimental settings with simulated and real-world data, the BCT-based methods were found to give results as good or better than state-of-the-art techniques. Moreover, they naturally also provide quantitative uncertainty estimates for all the results obtained. In particular, they were very effective in DNA segmentation problems, which form a key class of applications.

The main limitation of the BCT-based methods is the same as that of the BCT framework upon which they are built, namely, that they are only effective with data that take on only a small number of possible values, typically no larger than 15 or 20. Therefore, an important direction for further work is to consider extensions that would work effectively with large (or continuous) alphabets, particularly in the case of natural language processing. Another limitation is that our methods are all “offline” and can only detect change-points after the entire time series has been observed. Therefore, another interesting direction for future work is the development of sequential methods, particularly in connection with timely applications related to online security.

## References

- R.P. Adams and D.J.C. MacKay. Bayesian online changepoint detection. *arXiv e-prints*, 0710.3742 [stat.ML], October 2007.
- S. Aminikhanghahi and D. Cook. A survey of methods for time series change point detection. *Knowl. Inf. Syst.*, 51(2):339–367, September 2017.
- D. Barry and J. A. Hartigan. A Bayesian analysis for change point problems. *J. Amer. Statist. Assoc.*, 88(421):309–319, 1993.
- R.J. Boys and D.A. Henderson. A Bayesian approach to DNA sequence segmentation. *Biometrics*, 60(3):573–581, September 2004.
- J.V. Braun and H.G. Müller. Statistical methods for DNA sequence segmentation. *Statist. Sci.*, 13(2):142–162, 1998.
- J.V. Braun, R.K. Braun, and H.G. Müller. Multiple changepoint fitting via quasilielihood, with application to DNA sequence segmentation. *Biometrika*, 87(2):301–314, 2000.
- P. Bühlmann and A.J. Wyner. Variable length Markov chains. *Ann. Statist.*, 27(2):480–513, April 1999.
- W. Cai, S. Borlace, M. Lengaigne, P. Rensch, M. Collins, G. Vecchi, A. Timmermann, A. Santoso, M. McPhaden, L. Wu, M. England, G. Wang, E. Guilyardi, and F.F. Jin. Increasing frequency of extreme El Niño events due to greenhouse warming. *Nature Climate Change*, 4(2):111–116, 2014.
- P. Cashin, K. Mohaddes, and M. Raissi. Fair weather or foul? The macroeconomic effects of El Niño. *Journal of International Economics*, 106(C):37–54, 2017.
- V. Chandola, A. Banerjee, and V. Kumar. Anomaly detection for discrete sequences: A survey. *IEEE Trans. Knowl. Data Eng.*, 24(5):823–839, May 2012.
- G.A. Churchill. Stochastic models for heterogeneous DNA sequences. *Bulletin of Mathematical Biology*, 51(1):79–94, 1989.
- G.A. Churchill. Hidden Markov chains and the analysis of genome structure. *Computers & Chemistry*, 16(2):107–115, 1992.
- K. Clark, I. Karsch-Mizrachi, D.J. Lipman, J. Ostell, and E.W. Sayers. GenBank. *Nucleic Acids Research*, 44(D1):D67–D72, January 2016. Online at: [www.ncbi.nlm.nih.gov](http://www.ncbi.nlm.nih.gov).
- P. Fearnhead. Exact and efficient Bayesian inference for multiple changepoint problems. *Stat. Comput.*, 16(2):203–213, 2006.
- P.J. Green. Reversible jump Markov chain Monte Carlo computation and Bayesian model determination. *Biometrika*, 82(4):711–732, December 1995.
- M. Gupta and J.S. Liu. Discussion of “A Bayesian approach to DNA sequence segmentation”. *Biometrics*, 60(3):582–583, 2004.

- R. Gwadera, A. Gionis, and H. Mannila. Optimal segmentation using tree models. *Knowl. Inf. Syst.*, 15(3):259–283, May 2008.
- D. Han, F. Tsung, and J. Xian. On the optimality of Bayesian change-point detection. *Ann. Statist.*, 45(4):1375–1402, 2017.
- T. Jacob and R.K. Bansal. Sequential change detection based on universal compression algorithms. In *2008 IEEE International Symposium on Information Theory (ISIT)*, pages 1108–1112, Toronto, ON, July 2008.
- D.R. Juvvadi and R.K. Bansal. Sequential change detection using estimators of entropy & divergence rate. In *2013 National Conference on Communications (NCC)*, pages 1–5, New Delhi, India, March 2013.
- R.E. Kass and A.E. Raftery. Bayes factors. *J. Amer. Statist. Assoc.*, 90(430):773–795, 1995.
- A. Kehagias. A hidden Markov model segmentation procedure for hydrological and environmental time series. *Stochastic Environmental Research and Risk Assessment*, 18(2):117–130, April 2004.
- I. Kontoyiannis. Context-tree weighting and Bayesian Context Trees: Asymptotic and non-asymptotic justifications. *IEEE Trans. Inform. Theory*, 70(2):1204–1219, February 2024.
- I. Kontoyiannis, L. Mertzanis, A. Panotonoulou, I. Papageorgiou, and M. Skoularidou. Revisiting context-tree weighting for Bayesian inference. In *2021 IEEE International Symposium on Information Theory (ISIT)*, pages 2906–2911, Melbourne, Australia, July 2021.
- I. Kontoyiannis, L. Mertzanis, A. Panotonoulou, I. Papageorgiou, and M. Skoularidou. Bayesian Context Trees: Modelling and exact inference for discrete time series. *J. R. Stat. Soc. Series B*, 84(4):1287–1323, September 2022.
- W.M. Koolen and S. de Rooij. Universal codes from switching strategies. *IEEE Trans. Inform. Theory*, 59(11):7168–7185, 2013.
- S. Kovats, M. Bouma, S. Hajat, E. Worrall, and A. Haines. El Niño and health. *Lancet*, 362(9394):1481–1489, 2003.
- W. Li. DNA segmentation as a model selection process. In *Proceedings of the Fifth Annual International Conference on Computational Biology*, pages 204–210, Montréal, Quebec, April 2001.
- X. Liu, H. Jiang, Z. Gu, and J.W. Roberts. High-resolution view of bacteriophage lambda gene expression by ribosome profiling. *Proc. Natl. Acad. Sci. U.S.A.*, 110(29):11928–11933, 2013.
- V. Lungu, I. Papageorgiou, and I. Kontoyiannis. Bayesian change-point detection via context-tree weighting. In *2022 IEEE Workshop on Information Theory (ITW)*, Mumbai, India, November 2022.
- M. Mächler and P. Bühlmann. Variable length Markov chains: Methodology, computing, and software. *J. Comput. Grap. Stat.*, 13(2):435–455, 2004.

- N. Merhav. On the minimum description length principle for sources with piecewise constant parameters. *IEEE Trans. Inform. Theory*, 39(6):1962–1967, November 1993.
- N. Merhav and M. Feder. A strong version of the redundancy-capacity theorem of universal coding. *IEEE Trans. Inform. Theory*, 41(3):714–722, May 1995.
- I. Papageorgiou and I. Kontoyiannis. Hierarchical Bayesian mixture models for time series using context trees as state space partitions. *arXiv e-prints*, 2106.03023 [stat.ME], June 2021.
- I. Papageorgiou and I. Kontoyiannis. The posterior distribution of Bayesian context-tree models: Theory and applications. In *2022 IEEE International Symposium on Information Theory (ISIT)*, pages 702–707, Espoo, Finland, June 2022.
- I. Papageorgiou and I. Kontoyiannis. The Bayesian Context Trees State Space Model for time series modelling and forecasting. *arXiv e-prints*, 2308.00913 [stat.ME], August 2023.
- I. Papageorgiou and I. Kontoyiannis. Posterior representations for Bayesian Context Trees: Sampling, estimation and convergence. *Bayesian Analysis*, 19(2):501–529, June 2024.
- I. Papageorgiou, V. Lungu, and I. Kontoyiannis. BCT: Bayesian Context Trees for discrete time series. *R package version 1.1*, December 2020; *version 1.2*, May 2022. Available at [CRAN.R-project.org/package=BCT](https://CRAN.R-project.org/package=BCT).
- W.H. Quinn, V.T. Neal, and S.E. Antunez De Mayolo. El Niño occurrences over the past four and a half centuries. *Journal of Geophysical Research: Oceans*, 92(C13):14449–14461, 1987.
- C.E. Rasmussen and Z. Ghahramani. Occam’s razor. In T. Leen, T. Dietterich, and T. Tresp, editors, *Advances in Neural Information Processing Systems*, volume 13, Denver, CO, November 2000.
- V.B. Reddy, B. Thimmappaya, R. Dhar, K.N. Subramanian, B.S. Zain, J. Pan, P.K. Ghosh, M.L. Celma, and S.M. Weissman. The genome of Simian virus 40. *Science*, 200(4341):494–502, 1978.
- J. Rissanen. A universal prior for integers and estimation by minimum description length. *Ann. Statist.*, 11(2):416–431, June 1983a.
- J. Rissanen. A universal data compression system. *IEEE Trans. Inform. Theory*, 29(5):656–664, September 1983b.
- J. Rissanen. Complexity of strings in the class of Markov sources. *IEEE Trans. Inform. Theory*, 32(4):526–532, July 1986.
- J. Rissanen. Stochastic complexity. *J. R. Stat. Soc. Series B*, 49(3):223–239, 253–265, 1987. With discussion.
- C.P. Robert and G. Casella. *Monte Carlo statistical methods*. Springer-Verlag, New York, NY, second edition, 2004.
- J.C. Rotondo, E. Mazzoni, I. Bononi, M. Tognon, and F. Martini. Association between Simian virus 40 and human tumors. *Frontiers in Oncology*, 9:670, 2019.

- F. Sanger, A.R. Coulson, G.F. Hong, D.F. Hill, and G.B. Petersen. Nucleotide sequence of bacteriophage  $\lambda$  DNA. *Journal of Molecular Biology*, 162(4):729–773, 1982.
- G. Schwarz. Estimating the dimension of a model. *Ann. Statist.*, 6(2):461–464, March 1978.
- G.I. Shamir. On strongly sequential compression of sources with abrupt changes in statistics. In *2003 IEEE International Conference on Communications (ICC)*, volume 4, pages 2924–2927, Anchorage, AK, May 2003.
- G.I. Shamir and D.J. Costello. Asymptotically optimal low-complexity sequential lossless coding for piecewise-stationary memoryless sources. I. The regular case. *IEEE Trans. Inform. Theory*, 46(7):2444–2467, November 2000.
- G.I. Shamir and D.J. Costello. On the redundancy of universal lossless coding for general piecewise stationary sources. *Commun. Inf. Syst.*, 1(7):305–332, January 2001.
- G.I. Shamir and N. Merhav. Low-complexity sequential lossless coding for piecewise-stationary memoryless sources. *IEEE Trans. Inform. Theory*, 45(5):1498–1519, July 1999.
- K. Shimada, S. Saito, and T. Matsushima. An efficient Bayes coding algorithm for the non-stationary source in which context tree model varies from interval to interval. In *2021 IEEE Information Theory Workshop (ITW)*, pages 1–6, Kanazawa, Japan, October 2021.
- A.F.M. Smith and D.J. Spiegelhalter. Bayes factors and choice criteria for linear models. *J. R. Stat. Soc. Series B*, 42(2):213–220, 1980.
- A. Timmermann, J.M. Oberhuber, A. Bacher, M. Esch, M. Latif, and E. Roeckner. Increased El Niño frequency in a climate model forced by future greenhouse warming. *Nature*, 398(6729):694–697, 1999.
- J.A. Totterdell, D. Nur, and K.L. Mengersen. Bayesian hidden Markov models in DNA sequence segmentation using R: The case of simian vacuolating virus (SV40). *Journal of Statistical Computation and Simulation*, 87(14):2799–2827, 2017.
- K.E. Trenberth. The definition of El Niño. *Bulletin of the American Meteorological Society*, 78(12):2771–2778, 1997.
- C. Truong, L. Oudre, and N. Vayatis. Selective review of offline change point detection methods. *Signal Processing*, 176:107299, February 2020.
- G.J.J. van den Burg and C.K.I. Williams. An evaluation of change point detection algorithms. *arXiv e-prints*, [2007.14900 stat.ML], March 2020.
- J. Veness, K.S. Ng, M. Hutter, and M.H. Bowling. Context tree switching. In *2012 Data Compression Conference*, pages 327–0336, April 2012.
- J. Veness, M. White, M. Bowling, and A. György. Partition tree weighting. In *2013 Data Compression Conference*, pages 321–330, March 2013.
- A. Verma and R.K. Bansal. Sequential change detection based on universal compression for Markov sources. In *2019 IEEE International Symposium on Information Theory (ISIT)*, pages 2189–2193, Paris, France, July 2019.



- B. Wang, X. Luo, Y.M. Yang, W. Sun, M.A. Cane, W. Cai, S.W. Yeh, and J. Liu. Historical change of El Niño properties sheds light on future changes of extreme El Niño. *Proc. Natl. Acad. Sci. U.S.A.*, 116(45):22512–22517, 2019.
- F.M.J. Willems. Coding for a binary independent piecewise-identically-distributed source. *IEEE Trans. Inform. Theory*, 42(6):2210–2217, November 1996.
- F.M.J. Willems. The context-tree weighting method: Extensions. *IEEE Trans. Inform. Theory*, 44(2):792–798, March 1998.
- F.M.J. Willems, Y.M. Shtarkov, and T.J. Tjalkens. The context tree weighting method: Basic properties. *IEEE Trans. Inform. Theory*, 41(3):653–664, May 1995.
- K. Yamanishi and S. Fukushima. Model change detection with the MDL principle. *IEEE Trans. Inform. Theory*, 64(9):6115–6126, September 2018.

# Appendix

## A MCMC acceptance probability

The ratio  $r((\ell, \mathbf{p}), (\ell', \mathbf{p}'))$  in the acceptance probability of the MCMC sampler in Section 3.2 is given by:

$$\frac{P(x|\mathbf{p}', \ell')}{P(x|\mathbf{p}, \ell)} \times \frac{\prod_{j=0}^{\ell'} (p'_{j+1} - p'_j - 1)}{\prod_{j=0}^{\ell} (p_{j+1} - p_j - 1)} \times \begin{cases} \frac{2(n-2)}{(n-3)(n-4)}, & \text{if } \ell = 0; \\ \frac{(n-3)(n-4)}{2(n-2)}, & \text{if } \ell = 1, \ell' = 0; \\ \frac{3(2\ell_{\max}+1)(n-\ell_{\max}-1)}{(n-2\ell_{\max}-2)(n-2\ell_{\max}-1)}, & \text{if } \ell = \ell_{\max} - 1, \ell' = \ell_{\max}; \\ \frac{(n-2\ell_{\max}-2)(n-2\ell_{\max}-1)}{3(2\ell_{\max}+1)(n-\ell_{\max}-1)}, & \text{if } \ell = \ell_{\max}, \ell' = \ell_{\max} - 1; \\ \frac{(n-2\ell-2)(n-2\ell-1)}{2(2\ell+1)(n-\ell-1)}, & \text{if } \ell' = \ell - 1, \ell \neq 1, \ell_{\max}; \\ \frac{2(2\ell'+1)(n-\ell'-1)}{(n-2\ell'-2)(n-2\ell'-1)}, & \text{if } \ell' = \ell + 1, \ell' \neq 1, \ell_{\max}; \\ 1, & \text{otherwise.} \end{cases}$$

## B Maximum number of change-points

Results of the experiments in the last part of Section 4.2.2. In both cases,  $N = 300,000$  MCMC samples were obtained, with the first 30% of the samples being discarded as burn-in.

## C Empirical running times

	Dataset with $n = 300$							
$\ell_{\max}$	10	25	50	100	150	200	280	293
Sampling time (seconds)	67.5	70	107	123	156	165	649	571
	Dataset with $n = 900$							
$\ell_{\max}$	10	25	100	300	500	600		
Sampling time (seconds)	114	143	138	759	3000	1791		

Table 4: MCMC sampling time for  $N = 300,000$  iterations of the BCT-based algorithm, for datasets 1 and 2 in Section 4.2.2.

## D Parameter values

The parameters of the four models depicted in Figure 4 are given below.

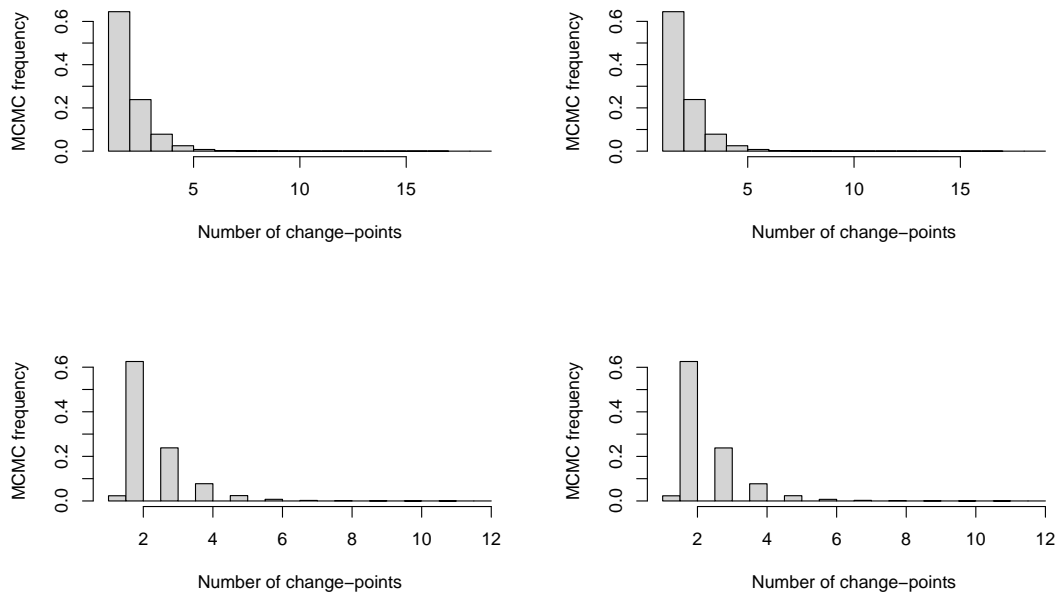


Figure 12: Posterior distribution of the number of change-points for dataset 1 in Section 4.2.2. From upper-left to lower-right,  $\ell_{\max} = 25, 100, 250, 293$ .

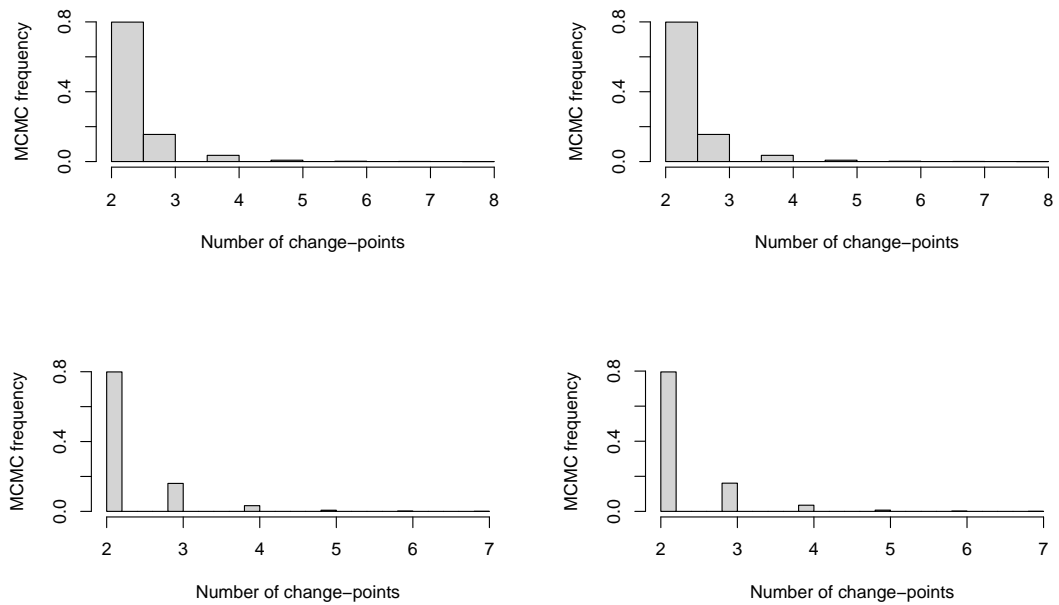


Figure 13: Posterior distribution of the number of change-points for dataset 2 in Section 4.2.2. From upper-left to lower-right,  $\ell_{\max} = 10, 150, 300, 600$ .

	Running time (seconds)	
	BCT	Bayesian HMM
dataset 1 (HMM generated)	58	7967
dataset 2 (HMM generated)	34	7108
dataset 3 (VLMC generated)	96	18510
dataset 4 (VLMC generated)	103	18030

Table 5: Running time for 110,000 iterations of the BCT-based algorithm and the Bayesian HMM algorithm, for the four datasets in Section 4.2.4.

Model 1				Model 2			
Context $s$	Probability $P(j s)$			Context $s$	Probability $P(j s)$		
	$j = 0$	1	2		$j = 0$	1	2
0	0.3	0.4	0.3	0	0.4	0.5	0.1
2	0.5	0.3	0.2	2	0.4	0.4	0.2
10	0.2	0.5	0.3	10	0.4	0.2	0.4
11	0.1	0.4	0.5	11	0.2	0.4	0.4
121	0.7	0.2	0.1	12	0.6	0.1	0.3
122	0.4	0.2	0.4				
1200	0.6	0.1	0.3				
1201	0.3	0.5	0.2				
1202	0.4	0.1	0.5				

Model 3				Model 4			
Context $s$	Probability $P(j s)$			Context $s$	Probability $P(j)$		
	$j = 0$	1	2		$j = 0$	1	2
0	0.5	0.3	0.2		0.4	0.2	0.4
1	0.3	0.6	0.1				
2	0.3	0.2	0.5				

The parameters of the two models depicted in Figure 8 are given below.

Model 1					Model 2				
Context $s$	Probability $P(j s)$				Context $s$	Probability $P(j s)$			
	$j = 0$	1	2	3		$j = 0$	1	2	3
1	0.3	0.4	0.2	0.1	0	0.3	0.4	0.2	0.1
2	0.25	0.25	0.25	0.25	2	0.4	0.2	0.3	0.1
3	0.25	0.25	0.25	0.25	3	0.25	0.25	0.25	0.25
00	0.3	0.4	0.2	0.1	10	0.1	0.1	0.2	0.6
01	0.2	0.2	0.2	0.4	12	0.2	0.1	0.5	0.2
03	0.4	0.4	0.1	0.1	13	0.4	0.1	0.4	0.1
020	0.3	0.4	0.1	0.2	110	0.2	0.3	0.3	0.2
021	0.2	0.4	0.2	0.2	111	0.3	0.4	0.1	0.2
022	0.6	0.1	0.2	0.1	112	0.7	0.1	0.1	0.1
023	0.8	0.1	0	0.1	1130	0.5	0.5	0	0
					1131	0.4	0.3	0.1	0.2
					1132	0.2	0.2	0.4	0.2
					1133	0.3	0.2	0.2	0.3

## E Additional results

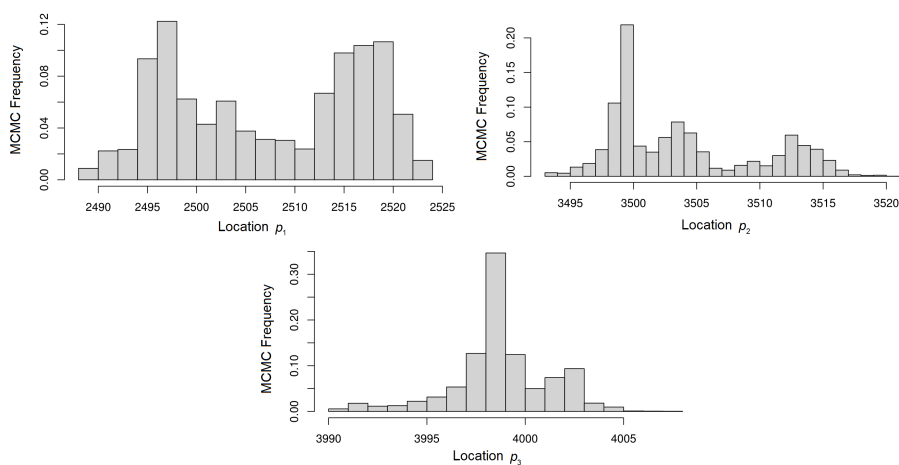


Figure 14: MCMC histograms of the posterior distribution of each change-point location in the simulated data example of Section 4.2.3.

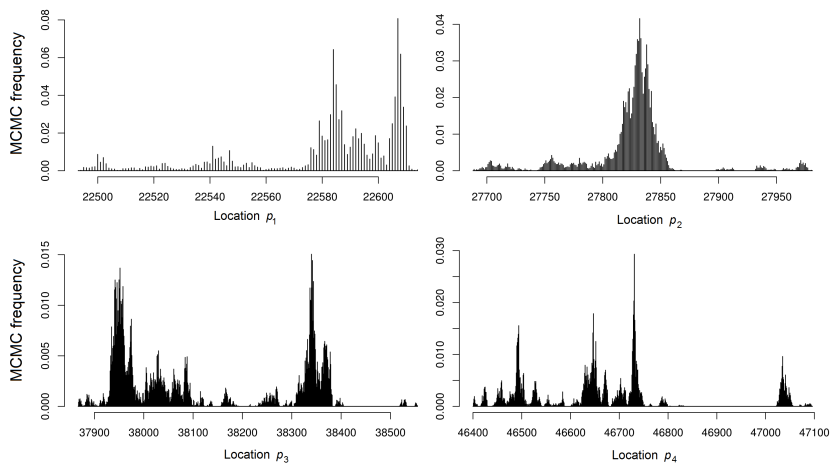


Figure 15: MCMC histograms of the posterior distribution of each change-point location in the bacteriophage lambda genome from Section 4.2.5.

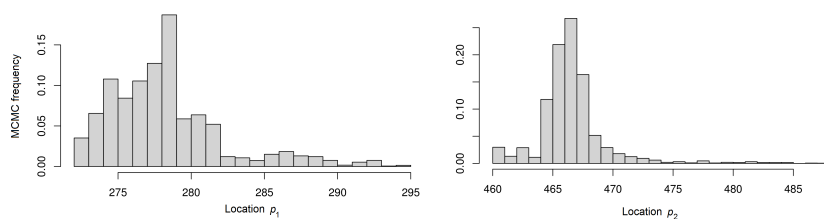


Figure 16: MCMC histograms of the posterior distribution of each change-point location in the meteorological data in Section 4.2.6.